Interaction between Surfaces with Adsorbed Polymers: Poor Solvents

Jacob Klein†
Cavendish Laboratory, Cambridge, England CB3 0HE
Philip Pincus*
ESPCI, 75231 Paris, France, and Department of Physics, University of California, Los Angeles, Los Angeles, California 90024. *Received January 11, 1982*

ABSTRACT: We analyze the interaction between planar surfaces carrying *irreversibly* adsorbed polymers under poor-solvent conditions. In particular, we consider the situation where the incubation polymer volume fraction ϕ_b is in the single-phase regime but the adsorption profile near an interface constrains the system to locally pass through the biphasic region of the bulk phase diagram. In contrast to good-solvent conditions, where the forces between plates separated by a narrow gap ($2h$) are repulsive, we find in poor solvents a mechanical equilibrium, i.e., short-range repulsion (force varying as h^{-3}) and a longer range attractive domain. The attractive interactions occur when the interfacial region is dominated by polymer concentrations that are unstable under bulk conditions. This behavior is both qualitatively and quantitatively in good agreement with recent observations on interactions between mica surfaces bearing adsorbed polystyrene in a cyclohexane medium.

I. Introduction

Colloidal suspensions are often protected against aggregation by steric stabilization with adsorbed polymers.[1] The required conditions for stabilization are, broadly speaking, that (1) the colloidal particles form an adsorptive substrate for the polymer in the particular solvent used and (2) the solvent is a good solvent for the polymer. Condition 1 ensures that the particles are coated with the polymer and condition 2 that the polymer–polymer interactions are repulsive. Then when two suspended particles approach one another (Figure 1) the repulsive polymer "bumpers" oppose the long-range van der Waals attraction[2] and may thus prevent aggregation and subsequent flocculation. Indeed some recent direct measurements of the force between surfaces with adsorbed polymer layers[3-5] under good-solvent conditions have demonstrated repulsive interactions increasing in strength monotonically with decreasing interfacial separation.

On the theoretical side, the situation is rather complex. The possibility of a polymer bridging the interfacial gap (Figure 1) adds an attractive interaction, which competes with the bumper effect. Indeed de Gennes[6b] has shown that in strict thermodynamic equilibrium the net force is always *attractive*. This is because under good-solvent conditions the bumper effect is reduced for narrow gaps by polymer desorption, which never allows the polymer concentration within the gap to become elevated. However, under most experimental conditions a polymer chain is bound to the interface by an energy greatly exceeding k_BT (the high polymer molecular weight ensures that even for a weak adsorption energy per monomer the adsorption energy per chain may be large), which, coupled with slow polymer diffusion, leads to effectively irreversible adsorption. Then if the surfaces are incubated in the polymer solution at large separation, the surface excess Γ

$$\Gamma = a^{-3}\int_0^\infty [\phi(z) - \phi_b]\, dz \qquad \text{(I.1)}$$

[$\phi(z)$ is the polymer volume fraction at a distance z from the interface, and ϕ_b is the corresponding bulk value] remains *constant* when the surfaces approach. Then, the polymer chains are indeed squeezed between the walls and the excluded volume repulsions come into play. Using mean field theory for the polymer adsorption[7,8] to investigate the steric stabilization[9] with the constrained coverage Γ leads to cancellation between the excluded volume repulsion and the bridging attraction.[6b] However, a more sophisticated approach[6b] that employs the correct static scaling exponents for good solvents leads to monotonic repulsive forces, consistent with the good-solvent experiments.[3-5]

More recently, one of us[10] has studied the force between mica surfaces with adsorbed polystyrene in cyclohexane under poor-solvent conditions, i.e., conditions that would lead to flocculation of sterically stabilized colloidal particles.[16] The experiments were performed below the Θ temperature of the bulk polystyrene–cyclohexane solution. The force was found to change sign; i.e., there exists an equilibrium separation. There is a strong short-range repulsion and an intermediate-range attraction, which becomes small at plate separations corresponding to twice the polymer radius of gyration. The purpose of this study is to extend the de Gennes[6b] analysis of the force between plates with adsorbed polymers to this poor-solvent situation.

In the next section, we review the Flory–Huggins theory for the phase diagram of a polymer in a poor solvent. In particular, we focus on the mean field structure of the dilute solution–semidilute solution interface in the biphasic region. Then in section III we consider adsorption on a single interface when the bulk solution is dilute, i.e., single phase, but the adsorption constrains the polymer density profile to pass through the biphasic region of the bulk phase diagram. It is precisely this density range, which is dominated by attractive forces between the monomeric units (negative second virial coefficient), that leads to the intermediate-range attractive force between the micas. This force between the plates is studied in section IV, and in section V we make a critical comparison between some predictions of our model and the results of the experimental study.[10]

II. Flory–Huggins Theory for a Polymer in a Poor Solvent

Let us consider a monodisperse polymer solution (DP = N) inscribed on a Flory–Huggins lattice (lattice constant a). The thermodynamics of the demixing in a poor solvent may be described in terms of a free energy per site, which may be written as a virial expansion:[11]

$$F_0/T = \frac{\phi}{N}\ln\phi - \frac{1}{2}v\phi^2 + \frac{1}{6}w\phi^3 + \ldots \qquad \text{(II.1)}$$

* To whom correspondence should be addressed at the University of California, Los Angeles.
† Also: Polymer Department, The Weizmann Institute, Rehovot, Israel.

0024-9297/82/2215-1129$01.25/0

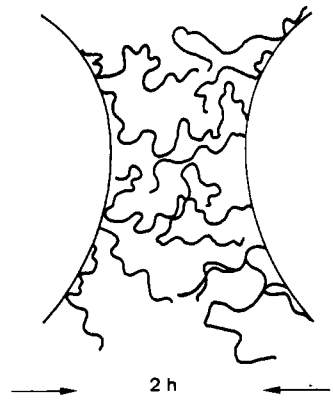

Figure 1. Schematic representation of two colloidal surfaces with adsorbed polymers near contact. Note the increased polymer density in the region of closest approach and the possibility of bridging when the separation ($2h$) is inferior to two polymer radii R, i.e., when $h < R$.

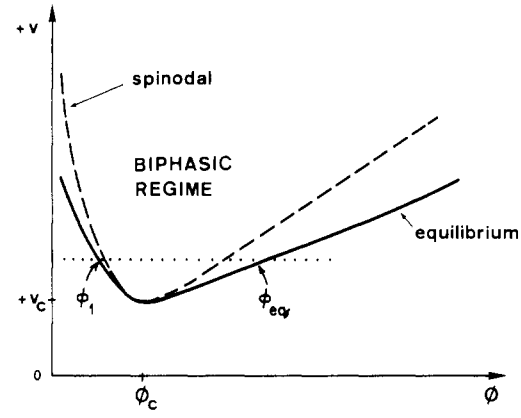

Figure 2. Poor-solvent side of the Flory–Huggins phase diagram for a polymer solution. The dashed curve is the spinodal line and the continuous curve gives the equilibrium concentrations of the two phases when the global concentration is in the biphasic region.

The first term describes the translation entropy per chain; with $v > 0$ the second virial coefficient is negative (i.e., $T < \Theta$) and we assume the third virial coefficient w to be a positive constant of order unity.[8] The spinodal line that delineates the unstable single-phase regime is determined by the condition that the osmotic compressibility $[\kappa^{-1} = a^{-3}\phi(\partial^2 F/\partial\phi^2)]$ diverges, which from (II.1) yields

$$v_s = (N\phi)^{-1} + w\phi \tag{II.2}$$

Then $v_s(\phi)$ (Figure 2) separates the stable and unstable homogeneous phase regions. The critical point is at $\phi_c = (Nw)^{-1/2}$ and $v_c = 2(w/N)^{1/2}$. Note that for polymers ($N \gg 1$), the dilute phase ($\phi < \phi_c$) is always *very* dilute; i.e., $\phi < \phi^*$ (ϕ^*, which is the concentration at which polymers begin to overlap, is of order ϕ_c in the Θ region). The equilibrium curve is determined by equating the chemical potentials $[\mu = a^{-3}(\partial F/\partial\phi)]$ and osmotic pressures $[\pi = \phi^2 a^{-3}(\partial/\partial\phi\ (F/\phi))]$ in the two phases. Not too close to the critical point, the dilute phase is very dilute and we may write $\pi(\phi_1) \approx 0 = \pi(\phi_{eq})$, where ϕ_1 and ϕ_{eq} are the respective concentrations on the dilute and semidilute branch of the coexistence curve (Figure 2). This gives

$$\phi_{eq} \simeq {}^3/_2(v/w) \tag{II.3}$$

The corresponding chemical potential is

$$(a^3/T)\mu_{eq} \simeq -v\phi_{eq}[1 - {}^1/_2(w/v)\phi_{eq}] = -{}^3/_8(v^2/w) \tag{II.4}$$

We now turn to a review of the structure of the interface between the coexisting dilute and semidilute phases. This

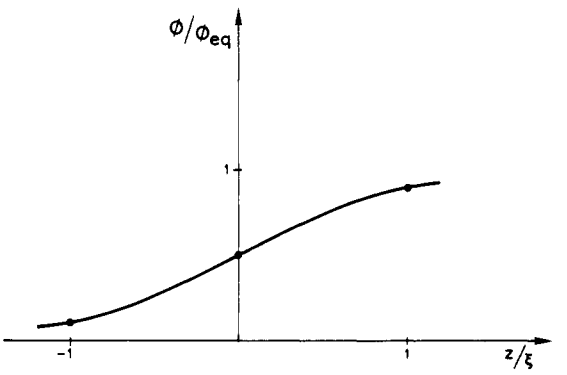

Figure 3. Sketch of the density profile of the dilute–semidilute polymer solution interface.

is accomplished by augmenting the free energy (II.1) with a term that allows for slow spatial variations,[8] in direct analogy with the interfacial structure in segregated polymer blends[12]

$$F = F_0 + (T/24)\phi^{-1}(a\nabla\phi)^2 \tag{II.5}$$

Following the Cahn[13] approach[6b] for the interfacial energy γ, we write

$$\gamma = \int_{-\infty}^{\infty} dz\ [F(\phi)a^{-3} - \mu_{eq}\phi + \pi_{eq}] \tag{II.6}$$

where the term in square brackets in the integral represents the free energy *difference* needed to create unit volume of composition ϕ from a reservoir of osmotic pressure π_{eq} and chemical potential μ_{eq} (suitably augmented by the gradient term, eq II.5). In terms of the mean field order parameter $\psi(z)[\phi(z) = \psi^2(z)]$, (II.6) becomes

$$\gamma \simeq (T/a^3)\int_{-\infty}^{\infty} dz \left[-\frac{1}{2}v\psi^4 + \frac{1}{6}w\psi^6 + \frac{3}{8}(v^2/w)\psi^2 + \frac{a^2}{6}\left(\frac{d\psi}{dz}\right)^2 \right] \tag{II.7}$$

Note that the use of ψ simplifies the gradient term and we have neglected the small osmotic pressure. It is convenient (1) to transform to a dimensionless length $x = z/\xi$, where ξ is the Edwards mean field correlation length[14] on the equilibrium curve $[\xi = a({}^3/_2 v\phi_{eq})^{-1/2}]$, and (2) to measure the order parameter ψ in terms of its value on the equilibrium curve ψ_{eq} ($\psi_{eq} = \phi_{eq}{}^{1/2}$). Then, defining $y = \psi/\psi_{eq}$

$$\gamma = \frac{3}{8}(T/a^2)v^2 w^{-3/2}\int_{-\infty}^{\infty} dx \left[y^2 - 2y^4 + y^6 + \left(\frac{dy}{dx}\right)^2 \right] \tag{II.8}$$

The Euler–Lagrange equation that gives the interfacial profile $y(x)$ is

$$d^2y/dx^2 = y - 4y^3 + 3y^5 \tag{II.9}$$

and has a first integral

$$dy/dx = (y^2 - 2y^4 + y^6)^{1/2} \tag{II.10}$$

where we have chosen the positive root that places the semidilute phase ($y \to 1$) at the right (Figure 3). Note that the boundary condition that the slope dy/dx vanishes in both phases ($y = 0, 1$) is obeyed. Choosing the origin at the midpoint (II.10) yields the profile (Figure 3)

$$\phi/\phi_{eq} = {}^1/_2[1 + \text{th}\ (z/\xi)] \tag{II.11}$$

and the corresponding interfacial energy

$$\gamma = {}^{1}/_{12}(T/\xi^2)w^{-1/2} \qquad \text{(II.12)}$$

The central result of this section is the profile (II.11); the interfacial thickness is $\xi = {}^{2}/_{3}(a/v)w^{1/2}$. Substituting from (II.3) we have $\xi \simeq aw^{-1/2}/\phi_{eq}$; for example, for polystyrene in cyclohexane a few degrees below the critical temperature, $\phi_{eq} \simeq 0.2$,[17] so that the interfacial thickness is of the order of a few polymer segments.

III. Adsorption in a Poor Solvent

We now consider polymer adsorption on either a free surface or a solid interface under the poor-solvent conditions depicted in Figure 2. Our approach is a straightforward extension of the Cahn–de Gennes[6a] method for good and Θ solvents. Thus, we limit our attention to the situation $v > v_c$ and (for simplicity) restrict the bulk solution to be in a homogeneous phase. For weak adsorption, the Cahn–de Gennes[6a] interfacial energy is

$$\gamma - \gamma_0 = -\gamma_1\phi_s + \int_0^\infty [F(\phi)/a^3 - \mu_b\phi + \pi_b]\, dz \qquad \text{(III.1)}$$

where z is the distance from the surface measured into the polymer solution, the integral is similar to the phase boundary energy (II.6) but with μ_b and π_b respectively the bulk chemical potential and osmotic pressure, γ_0 is the pure solvent–surface interfacial energy, γ_1 (>0) describes the "sticking" energy of a monomeric unit to the wall, and ϕ_s is the polymer volume fraction at the surface; i.e., $\phi_s = \phi(0)$. The essential assumption in the form of the "sticking" energy is that the adsorption is weak (i.e., $\gamma_1 a^2/T < 1$), which restricts the coverage to be low ($\phi_s < 1$). Deviations from this approximation could, of course, be studied by augmenting this term with a power series expansion of ϕ_s. A further important assumption implicit in (III.1) is that the long-range tail ($\sim Hz^{-3}$, where H is a Hamaker constant) of van der Waals interactions between the surface and the monomers is not significant. A consideration of the problem shows that the effect of even large Hamaker constants is essentially only to renormalize γ_1.[6a] It is important to recognize that weak binding is consistent with irreversible adsorption because though the adsorption energy per monomer is small (compared to thermal energies) and thus the sticking probability is low, the sticking energy per polymer chain may be large. This sticking energy is $U \sim Nf\gamma_1 a^2$, where f is the sticking probability per monomer and is of order $\gamma_1 a^2/T$, giving

$$U/T \simeq N(\gamma_1 a^2/T)^2 \qquad \text{(III.2)}$$

Typically, $\gamma_1 a^2/T \sim 10^{-2}$–$10^{-1}$, $N \sim 10^4$–10^5, and the situation of both weak "sticking" or binding and irreversible adsorption ($U/T \gg 1$) is not unusual.

Under these conditions, there exist two cases: the bulk polymer concentration is in the semidilute range ($\phi_b > \phi_{eq}$); the bulk concentration is dilute, i.e., to the left of the dilute branch of the equilibrium curve of Figure 2. For the semidilute case ($\phi_b > \phi_{eq}$) the situation is very similar to adsorption in a Θ solvent considered in ref 6a and we will not discuss this further.[4,5] The more novel case arises when the bulk concentration is very dilute but the attractive wall tends to push the local polymer concentration in the vicinity of the wall into the unstable region. Not too close to the critical point, $\phi_b \ll \phi^*$, the bulk osmotic pressure is small and to a good approximation we may assume $\pi_b \simeq 0$. On the other hand, the chemical potential is logarithmically large, $\mu_b \simeq (T/Na^3) \ln \phi_b$.

Then rewriting the interfacial energy (III.1) in terms of the order parameter ψ ($=\phi^{1/2}$), we obtain

$$\gamma - \gamma_0 = -\gamma_1\psi_s^2 + (T/a^3)\int_0^\infty dz \left[-\frac{1}{2}v\psi^4 + \frac{1}{6}w\psi^6 - (N^{-1} \ln \psi_b^2)\psi^2 + \frac{a^2}{6}\left(\frac{d\psi}{dz}\right)^2 \right] \qquad \text{(III.3)}$$

It is convenient to use the same variables as in section II; the reduced order parameter is $y = \psi/\psi_{eq}$ and distances are measured in terms of the correlation length on the semidilute branch of the equilibrium curve, $x = z/\xi$. The interfacial energy then takes the form

$$(\gamma - \gamma_0)(\gamma_1\phi_{eq})^{-1} = -y_s^2 + \sigma^{-1}\int_0^\infty dx \left[\beta^2 y^2 - 2y^4 + y^6 + \left(\frac{dy}{dx}\right)^2 \right] \qquad \text{(III.4)}$$

where σ is a dimensionless coupling constant

$$\sigma = 6\gamma_1 a\xi/T \qquad \text{(III.5)}$$

and the parameter β is

$$\beta^2 = \ln \phi_b/\ln \phi_1 > 1 \qquad \text{(III.6)}$$

with ϕ_1 equal to the monomer density on the dilute branch of the equilibrium curve (Figure 2). For $\phi_b < \phi_1$, $\beta > 1$ and will be very close to 1 for all practical cases. It is instructive to recast β in terms of the size of the polymer molecule. We first note the equality of the chemical potentials $\mu(\phi_1)$ and $\mu(\phi_{eq}) \equiv \mu_{eq}$ on either side of the coexistence curve (Figure 2). Also since $\phi_1 \ll \phi^* \ll 1$, the chemical potential will be logarithmically large, $\mu(\phi_1) \simeq (T/Na^3) \ln \phi_1$, and so

$$\mu(\phi_1) = \frac{T}{Na^3} \ln \phi_1 = \mu(\phi_{eq}) = -\frac{3}{8}\frac{T}{a^3}\frac{v^2}{w}$$

from (II.4). Thus

$$\ln \phi_1 = -\frac{3}{8}\frac{Nv^2}{w} = -\frac{Na^2}{6\xi^2}$$

Substituting for $\ln \phi_1$ in (III.6), we find

$$\beta = (\xi/R_g)(\ln \phi_b^{-1})^{1/2} \qquad \text{(III.6')}$$

where R_g is the unperturbed radius of gyration of the polymer $= {}^{1}/_{6}(Na^2)^{1/2}$. Returning to eq III.4, we find the first integral of the Euler–Lagrange equation obtained by setting $\delta\gamma/\delta y = 0$ is

$$(dy/dx)^2 = y^6 - 2y^4 + \beta^2 y^2 \qquad \text{(III.7)}$$

Then reinserting (III.7) into (III.4), we find an implicit dependence of the interfacial energy on surface density

$$(\gamma - \gamma_0)(\gamma_1\phi_{eq})^{-1} = -y_s^2 + (2/\sigma)\int_0^{y_s} |dy/dx|\, dy \qquad \text{(III.8)}$$

and minimizing this function with respect to y_s we obtain the Cahn–de Gennes boundary condition on y_s

$$2y_s = \frac{2}{\sigma}\left|\frac{dy}{dx}\right|_{y_s} \qquad \text{(III.9)}$$

This equation has a real solution for ϕ_s only when

$$\sigma > \sigma^* = (\beta^2 - 1)^{1/2} \qquad \text{(III.10)}$$

Not too close to the critical point σ^* is a constant of order unity. For $\sigma \gg \sigma^*$ the minimum of (III.8) is at

$$\phi_s/\phi_{eq} \simeq 1 + \sigma \qquad \text{(III.11)}$$

For $\sigma < \sigma^*$, the sticking energy cannot compensate the cost

in volume energy of deformation and there is no adsorption. If σ could be continuously varied, for example, as a function of temperature or surface treatment, we would predict a discontinuous jump in the surface concentration ($\Delta\phi_s \sim \phi_{eq}$) at $\sigma = \sigma^*$. For $\sigma \gg \sigma^*$, the surface tension is

$$\gamma - \gamma_0 \simeq -3\gamma_1(\gamma_1 a^2/T) \qquad \text{(III.12)}$$

The surface excess Γ, (I.1), becomes

$$\Gamma a^2 = w^{-1/2}\int_0^{y_*} y^2|dy/dx|^{-1}\,dy \qquad \text{(III.13)}$$

which, for $\sigma \gg \sigma^*$, is $\Gamma a^2 \simeq {}^1/_2 w^{-1/2} \ln [2\sigma(\beta - 1)^{-1}]$. In practice then, surface excess Γa^2 is of order unity.

The density profile $\phi(z)$ in the vicinity of the surface is complex and is given from (III.7) by the implicit relation

$$2z/\xi = \int_{y^2}^{y_*^2} \frac{dx}{x}(x^2 - 2x + \beta^2)^{-1/2} \qquad \text{(III.14)}$$

For $\sigma \gg \sigma^*$ and $\phi(z)/\phi_{eq} \gg 1$, the profile is

$$\phi(z) = \frac{6(\gamma_1 a^2/T)}{1 + z/D} \qquad \text{(III.15)}$$

where the extrapolation length $D = T/12\gamma_1 a \gg a$. The monomer density falls to ϕ_{eq} at z_0

$$z_0 \simeq \frac{\xi}{2\beta} \ln \left\{ \frac{\beta(\beta^2 - 1)^{1/2} + (\beta^2 - 1)}{\beta - 1} \right\} \qquad \text{(III.16)}$$

$$= \frac{1}{2} R_g \left[\frac{\ln [(\beta(\beta^2 - 1)^{1/2} + (\beta^2 - 1))/(\beta - 1)]}{(\ln \phi_b^{-1})^{1/2}} \right] \qquad \text{(III.17)}$$

on substituting for ξ/β from (III.6′). If $\beta = 1 + \epsilon$, where $\epsilon \ll 1$ (often the case)

$$z_0 \simeq \frac{1}{2} R_g \frac{\ln ((2\epsilon)^{-1/2})}{(\ln (\phi_b^{-1}))^{1/2}} \qquad \text{(III.18)}$$

Note that for $\beta = 1$, i.e., the bulk density on the dilute branch of the coexistence curve, the density rests constant at ϕ_{eq}. For $2z_0 \geq z \geq z_0$, the density profile falls only logarithmically with z and finally for $z \gg z_0$, $\phi(z)$ falls exponentially to zero

$$\phi(z)/\phi_{eq} \simeq 2\beta^2[\beta(\beta^2 - 1)^{1/2} + (\beta^2 - 1)]^{-1} e^{-(z - z_0)/\alpha} \qquad z > 2z_0 \qquad \text{(III.19)}$$

where

$$\alpha = R_g[2(\ln \phi_b^{-1})^{1/2}]$$

(Figure 4).

The essential result of this section is that the adsorption profile in the poor-solvent regime ($v > v_c$) divides into three regions (Figure 4): an *inner* region $\phi > \phi_{eq}$ where the profile falls rapidly as $[1 + (z/D)]^{-1}$, a broad *central* plateau extending from z_0 to $2z_0$ where the density traverses the unstable part of the bulk phase diagram, and an *outer* region where the density falls exponentially ($\sim e^{-2z/\xi}$) toward the bulk value. The overall thickness of the adsorbed layer d may be defined as $d = \Gamma a^3/\phi_{eq}$ and is

$$d \simeq \frac{\xi}{2} \ln [2\sigma(\beta - 1)^{-1}] = \frac{\beta R_g}{2(\ln \phi_b^{-1})^{1/2}} \ln [2\sigma(\beta - 1)] > z_0 \qquad \text{(III.20)}$$

Thus the range of both the interesting plateau region z_0 and the overall thickness d is determined by the unperturbed polymer size R_g, which depends on $N^{1/2}$.

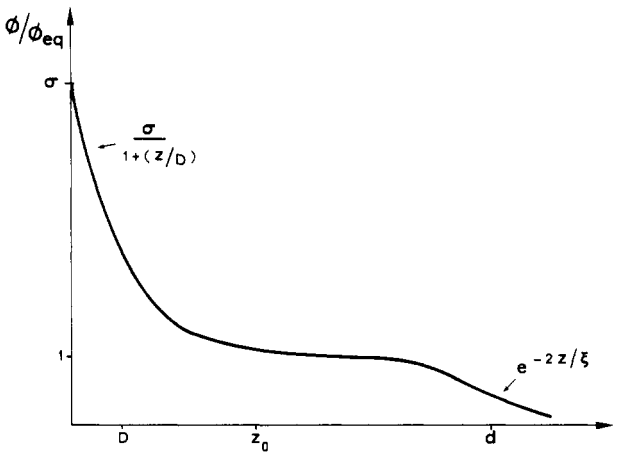

Figure 4. Sketch of the density profile at an adsorbing wall under poor-solvent conditions. Note the large plateau region in the vicinity of z_0, where the density is approximately ϕ_{eq}.

IV. Force between Plates with Adsorbed Polymers

We are now in a position to compute the force between two parallel plates with adsorbed polymers in poor solvents. This should enable us to make contact with the measurements of the force between mica cylinders with adsorbed polystyrene in cyclohexane (24 °C) investigated in ref 10. A novel feature of these results is that the potential energy associated with the interplane force is *not* monotonic; i.e., there exists an equilibrium separation. This is in contrast with polymer/good solvent couples where monotonic repulsive forces are both observed[3-5] and predicted.[6] The physical origin of the unusual attractive force is associated with the poor-solvent conditions. As we saw in section III, the plateau region of the single-plate adsorption profile passes through the unstable concentration regime of the bulk phase diagram. This concentration range is dominated by the negative second virial coefficient, signifying overall *attractive* interactions between polymer chains. Thus it is not surprising that when the separation between two parallel plates with adsorbed polymers corresponds to the plateau region, attractive forces between the plates develop. At smaller separations (less than z_0), repulsive forces associated with the positive third virial coefficient will dominate. We are then led to expect an *equilibrium* separation in the vicinity of z_0.

It is important to recall that polymer adsorption is generally irreversible provided that the extrapolation length D is smaller than the chain radius. Then it is necessary to specify the sample history when analyzing a particular experiment. We restrict our attention to the situation where two plates are incubated in a polymer solution at very large separation. This results in adsorbed layers with surface excess Γ, (III.13). The polymer solution is then washed; i.e., the solution is replaced by pure solvent. The irreversibly adsorbed polymer chains remain, maintaining the surface excess, Γ, nearly constant. The separation ($2h$) between the plates is slowly reduced and the force measured. We assume here that the motion is quasi-static so that the adsorption profiles may adjust to optimize the free energy with the constraint of irreversible adsorption.

Following the de Gennes[6b] approach, there is an augmented interfacial energy function $\tilde{\gamma}$ per plate which is a generalization of (III.1) to the constrained, two-interface problem

$$\tilde{\gamma} - \gamma_0 = -\gamma_1\phi_s + \frac{T}{a^3}\int_0^h \left| G'(\psi) + \frac{a^2}{6}\left(\frac{d\psi}{dz}\right)^2 \right| dz \qquad \text{(IV.1)}$$

where $\psi^2 = \phi$ as in section III. The functional $G'(\psi)$ is

$$G'(\psi) = -\tfrac{1}{2}v\psi^4 + \tfrac{1}{6}w\psi^6 + k'\psi^2 \qquad \text{(IV.2)}$$

where the constant k' is a Lagrange multiplier that is determined by the irreversible adsorption constraint that the surface excess remain fixed at its incubation value. This Lagrange multiplier term has the same dependence on the order parameter, ψ, as the chemical potential term in (III.1) so, following de Gennes,[6] we refer to k' as a pseudochemical potential.

Transforming to the same dimensionless variables (y, x) as in sections II and III

$$y = \psi/\psi_{eq}; \qquad x = z/\xi$$

(IV.1) becomes

$$\tilde{\gamma} - \gamma_0 = -\gamma_1\phi_{eq}y_s^2 + (Tw^{-1/2}/6\xi^2)\int_0^{h/\xi} dx\, [G(y) + (dy/dx)^2] \qquad \text{(IV.3)}$$

where

$$G(y) = y^6 - 2y^4 + ky^2 \qquad \text{(IV.4)}$$

and

$$k = 6k'(\xi/a)^2 \qquad \text{(IV.5)}$$

The Euler–Lagrange equation for the profile derived from (IV.3) is

$$(dy/dx)^2 = G(y) - G(y_m) \qquad \text{(IV.6)}$$

where $y_m = y(h/\xi)$ is the value of $y(x)$ at the midplane between the two plates. The term $G(y_m)$ ensures that the profile is symmetric about the midplane. Integrating (IV.6), we obtain the determining equation for y_m

$$h/\xi = \int_{y_m}^{y_s} dy\, [G(y) - G(y_m)]^{-1/2} \qquad \text{(IV.7)}$$

The pseudochemical potential is derived from the surface excess

$$\Gamma a^2 = a^{-1}\int_0^h \phi(z)\, dz = w^{-1/2}\int_0^{h/\xi} y^2\, dx = w^{-1/2}\int_{y_m}^{y_s} dy\, y^2[G(y) - G(y_m)]^{-1/2} \qquad \text{(IV.8)}$$

where Γ is given by (III.13). Finally, the contact density, y_s, is found by minimizing $\tilde{\gamma}$ (eq IV.3)

$$\sigma y_s = [G(y_s) - G(y_m)]^{1/2} \qquad \text{(IV.9)}$$

where the coupling constant σ is defined by (III.5). The coupled equations (IV.7) to (IV.9) together with $G(y)$, (IV.4), determine the three parameters k, y_s, and y_m, which completely fix the profile between the plates.

The pressure acting between the plates π_h is given by $\pi_h = -(\partial\tilde{\gamma}/\partial h)$ and is

$$\pi_h = -\frac{Tw^{-1/2}}{6\xi^3}G(y_m) \qquad \text{(IV.10)}$$

In principle, the set (IV.7) to (IV.9) may be solved numerically to yield $\pi_h(h)$. This is rather complex and we shall only show (i) that the de Gennes conjecture of h^{-3} repulsive force at close separation is correct and (ii) that at intermediate separations $2z_0 > h > z_0$ there are attractive forces yielding an equilibrium separation. In section V we shall also make further comparisons of the predictions of the model with experiment.

(i) Small Gaps ($h < D$). For small separations ($h < D$), the profile $\phi(z)$ is nearly uniform and we may neglect the gradient terms in (IV.3). The polymer volume fraction between the plates is then $\phi = \Gamma a^3/h$ ($>\phi_{eq}$). The interfacial energy is dominated by the third virial coefficient term, yielding

$$\gamma - \gamma_0 \simeq (Thw/6a^3)\phi^3 = (wT/6)(\Gamma a^2)^3h^{-2} \qquad \text{(IV.11)}$$

and a corresponding repulsive force

$$\pi_h = (wT/3)(\Gamma a^2/h)^3 \qquad \text{(IV.12)}$$

in agreement with de Gennes.[6b] Note that this force scales as $(\ln N)^3$ and is just the osmotic pressure exerted on the walls by the polymer chains confined in the gap.

(ii) Equilibrium Region. For separations h corresponding to the plateau region $z_0 \lesssim z \lesssim 2z_0$ of the single-interface adsorption profile, we expect the interplate force to be dominated by the attractive interactions between polymer chains in the unstable region. Thus we are led to expect an equilibrium separation z_{eq} (in the vicinity of z_0) where this attractive force is balanced by the repulsive osmotic pressure, which is dominant for small gaps.

If we let $y_\equiv = y_m(z_{eq})$, we must have $G(y_\equiv) = 0$, from (IV.10), or

$$k = y_\equiv^2(2 - y_\equiv^2) \qquad \text{(IV.13)}$$

The secular equation (IV.9) is easily solved to give

$$y_s^2 = 1 + (1 + \sigma^2 - k)^{1/2} \simeq \sigma \qquad \text{(IV.14)}$$

The pseudochemical potential k cannot exceed 1 (from (IV.13)), and, because we assume strong coupling ($\sigma \gg 1$), we find that at equilibrium $\phi_s \simeq \sigma\phi_{eq}$. The precise value of the pseudochemical potential determined by the constant surface excess requirement (IV.8) becomes, in equilibrium

$$\Gamma a^2 = w^{-1/2}\int_{y_\equiv}^{y_s} dy\, y(y^4 - 2y^2 + k)^{-1/2} \simeq \tfrac{1}{2}w^{-1/2}\ln[2\sigma(y_\equiv^2 - 1)^{-1}] \qquad \text{(IV.15)}$$

Equating this to the incubated surface excess (III.13) yields

$$y_\equiv^2 = \beta \gtrsim 1 \qquad \text{(IV.16)}$$

Thus the equilibrium position z_{eq} occurs slightly out of the unstable region. This is given from (IV.7) by

$$z_{eq}/\xi = \int_{y_\equiv}^{y_s} dy\, [G(y)]^{-1/2} \qquad \text{(IV.17)}$$

giving

$$z_{eq} \simeq \frac{\xi}{2\beta(2/\beta - 1)^{1/2}}\ln\left\{\frac{\beta - 1}{1 - [\beta(2 - \beta)]^{1/2}}\right\} \qquad \text{(IV.18)}$$

and by comparison with (III.16)

$$z_{eq} > z_0$$

The equilibrium separation exceeds z_0 for a single layer because of the superposition of the polymer densities associated with the two plates. For larger gaps ($h > z_{eq}$) the interaction between plates is attractive, becoming very small for $h \sim d$, where d is the interfacial layer thickness (III.16). The interplate force law is sketched in Figure 5.

V. Discussion and Concluding Remarks

We can now compare the calculations of the present paper with results for polystyrene in cyclohexane. To facilitate subsequent discussion we reproduce in Figure 6 the experimental force–distance profile $F(2h)$ between

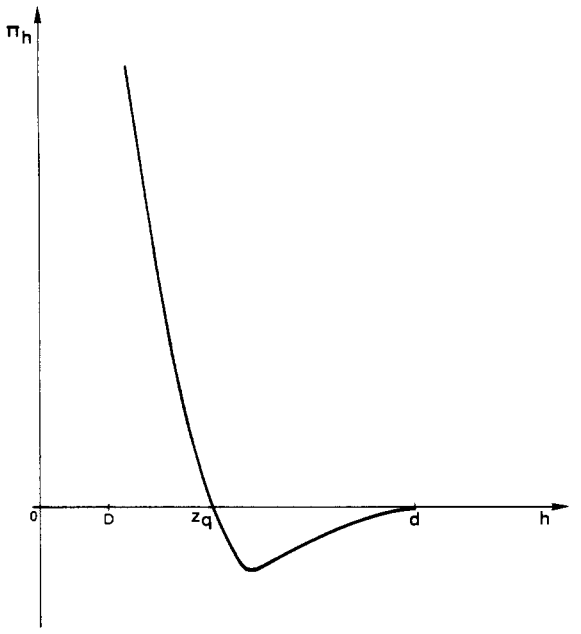

Figure 5. Sketch of the force between plates as a function of separation.

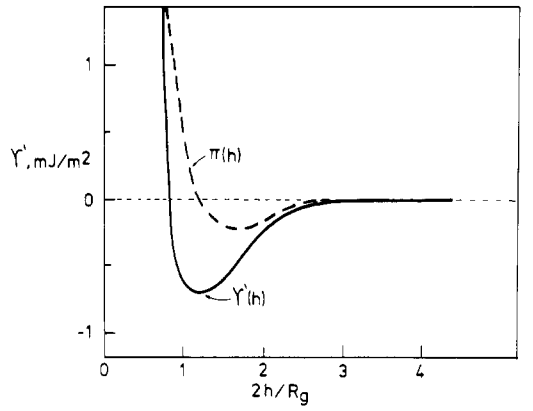

Figure 6. Interaction energy/area $\gamma'(h)$ between two flat mica plates bearing adsorbed polystyrene ($M = 6 \times 10^5$) a distance $2h$ apart in cyclohexane (solid line); based on data from ref 10, where the force profile $F(2h)$ between two curved mica surfaces (mean curvature radius = R_{mica}) was measured ($\gamma' = F/R_{mica}$ in the Derjaguin approximation). The pressure $\pi(h) \equiv \partial\gamma'/\partial h$ is also shown (broken line).

curved mica surfaces (radius of curvature = R_{mica}) bearing adsorbed polystyrene in cyclohexane at 24 °C. Details of the experiment are given in ref 10. The amount of polymer adsorbed, as determined in the same experiments,[10] is $\Gamma' \simeq 6$ mg·m^{-2} on each mica surface.[18] For simplicity, we draw in Figure 6 the *interaction energy* per unit area, γ', of *flat plates* at $2h$ in the Derjaguin approximation.[19] The pressure between flat plates a distance $2h$ apart is then

$$\pi(h) = \partial\gamma'/\partial h \qquad \text{(V.1)}$$

and the experimental $\pi(h)$ is indicated in Figure 6.

Comparing the experimental $\pi(h)$ in Figure 6 with the schematic $\pi(h)$ profile based on our calculations (Figure 5), we find qualitative agreement: in particular, we both predict and observe a nonmonotonic force between the adsorbed layers and the existence of an *equilibrium separation*, in contrast to the monotonic repulsion observed[3-5] and predicted[1,6,20] in good solvents.

Before making a more quantitative comparison, however, we should note that a number of inequalities on the various length scales must be satisfied for the validity of our calculations. These are as follows:

(*i*) *Weak Adsorption*: $a/D < 1$ [*or* $\gamma_1 a^2/T \ll 1$]. This is necessary in order that the simple linear form of the contact interaction ($\gamma_1\phi_s$) has meaning.

(*ii*) *Irreversible Adsorption*: $R = 6^{1/2}R_g \gg D$ [*or* $U/T \gg 1$, *eq III.3*]. This condition ensures that the adsorption energy per chain exceeds thermal energies. After incubation at large separations ($h \gg R$), when the walls approach one another, strict equilibrium would lead to chain desorption. The probability of activation over the barrier is proportional to $e^{-U/T}$ and is thus very small. Then we assume that during the time scale of the experiment this condition ($R \gg D$) ensures that the surface excess does not have time to readjust.

(*iii*) *Strong Coupling*: $\epsilon/D > 1$ [*i.e.*, $\sigma \gg 1$].

(*iv*) *Validity of Profile and Force Law*: $R \gtrsim z_{eq}, d$.

Bearing these conditions in mind, we now compare (a) z_{eq} and (b) d as predicted from our calculations with the corresponding experimental values (Figure 6).

(a) z_{eq}: from eq IV.18 and III.6′ we have

$$z_{eq} = \frac{1}{2}R_g\left\{\frac{1}{(\ln \phi_b^{-1})^{1/2}}\right\}\frac{1}{(2/\beta - 1)^{1/2}} \ln\left\{\frac{\beta - 1}{1 - (2\beta - \beta^2)^{1/2}}\right\} \qquad \text{(V.2)}$$

For polystyrene ($M = 6 \times 10^5$) in cyclohexane at 24 °C we find[21] $\phi_1 = (1.5 \pm 0.5) \times 10^{-4}$, and with $\phi_b = (7 \pm 2) \times 10^{-6}$ [10] we have

$$\beta = 1.16 \pm 0.04$$

Thus

$$2z_{eq} = (0.95 \pm 0.1)R_g \quad \text{(calcd, eq V.2)} \qquad \text{(V.3a)}$$

and

$$2z_{eq} = (1.1 \pm 0.1)R_g \quad \text{(exptl, Figure 6)} \qquad \text{(V.3b)}$$

The agreement, in the absence of adjustable parameters, is very good.

(b) To obtain d we use eq III.20 and III.13:

$$d \simeq \frac{\beta R_g}{(\ln \phi_b^{-1})^{1/2}}\Gamma a^2 w^{-1/2} \qquad \text{(V.4)}$$

and our experimentally measured value[10,18] for Γ' to obtain Γa^2, giving

$$2d \simeq w^{1/2}(2R_g) \quad \text{(calcd, eq V.4)} \qquad \text{(V.5a)}$$

and

$$2d \simeq 2 - 3R_g \quad \text{(exptl, Figure 6)} \qquad \text{(V.5b)}$$

We recall that w is of order unity.

Using these values of β and Γ', we may also readily show that the inequalities i–iv above are well obeyed for the polystyrene–cyclohexane system at 24 °C.

It is appropriate to note at this point that the results of Figure 6 ($M = 6 \times 10^5$) have been extended[22] to a polystyrene of different molecular weight ($M = 10^5$): here, too, a nonmonotonic $\pi(h)$ profile is observed, with $z_{eq} \simeq R_g$ and $d \simeq 2R_g$, in agreement with the predictions of our calculations.

To conclude: We have shown that when polymers are adsorbed on a substrate from a solvent below the Θ temperature, the resulting force between plates with adsorbed layers is nonmonotonic and should have an equilibrium separation, i.e., a position where the force is zero. This is very different from the monotonic repulsion observed[3-5] and calculated[1,6,20] for good solvents but is in good qualitative and quantitative agreement with the force profiles between adsorbed polystyrene layers in cyclohexane below the critical temperature. The theory also makes definite

predictions on the temperature and molecular weight dependence of the force law, which are currently being tested experimentally.

Acknowledgment. P.P. is pleased to express his thanks to Professors P.-G. de Gennes and T. Witten for helpful conversations. He has also benefited from several discussions with R. Cantor on polymer adsorption. J. Klein is grateful to Professor P. J. Flory for an illuminating remark and to Professor A. Silberberg for a useful discussion. We acknowledge partial support from the National Science Foundation.

References and Notes

(1) For a good review on steric stabilization see: Vincent, B. *Adv. Colloid Interface Sci.* **1974**, *4*, 193.
(2) Ninham, B. W.; Mahanty, J. "Dispersion Forces"; Academic Press: London, 1976.
(3) Lyklema, H.; Van Vliet, T. *Faraday Discuss. Chem. Soc.* **1978**, *No. 65*, 25.
(4) Cain, F. W.; Ottewill, R. H.; Smitham, J. B. *Faraday Discuss. Chem. Soc.* **1978**, *No. 65*, 33.
(5) Israelachvili, J. N.; Tandon, J. N.; White, L. R. *Nature (London)* **1979**, *277*, 120.
(6) (a) de Gennes, P.-G. *Macromolecules* **1981**, *14*, 1637. (b) *Ibid.* **1982**, *15*, 492.
(7) Jones, I. S.; Richmond, P. *J. Chem. Soc., Faraday Trans. 2* **1977**, *73*, 1062.
(8) de Gennes, P.-G. "Scaling Concepts in Polymer Physics"; Cornell University Press: Ithaca, N.Y., 1979.
(9) Moore, M. *J. Phys. A: Math., Nucl. Gen.* **1977**, *10*, 305.
(10) Klein, J. *Nature (London)* **1980**, *288*, 248.
(11) We use units with the Boltzmann constant taken to be unity.
(12) Helfand, E.; Tagami, Y. *J. Chem. Phys.* **1971**, *56*, 3592. *Ibid.* **1972**, *57*, 1812.
(13) Cahn, J. *J. Chem. Phys.* **1977**, *66*, 3667.
(14) Edwards, S. F. *J. Phys. A: Math., Gen. Nucl.* **1975**, *8*, 1670.
(15) If the wall is repulsive, the monomer density near the wall may enter the unstable region of the bulk phase diagram. This may be investigated by the method used here for a dilute solution and an attractive interface.
(16) Napper, D. H. *J. Colloid Interface Sci.* **1977**, *58*, 390.
(17) Schultz, A. R.; Flory, P. J. *J. Am. Chem. Soc.* **1952**, *74*, 4760.
(18) Recently, direct experiments of adsorption of polystyrene on mica at the Θ temperature using a microbalance technique have yielded similar values of the adsorbance.
(19) Derjaguin, B. V. *Koilloidn. Zh.* **1934**, *69*, 155.
(20) Scheutjens, J. M. H. M.; Fleer, G. J. *Adv. Colloid Interface Sci.*, in press.
(21) Klein, J., unpublished data.
(22) Klein, J. *Adv. Colloid Interface Sci.*, in press.

Monte Carlo Simulation of Protein Folding Using a Lattice Model

William R. Krigbaum* and Stephen F. Lin†

Gross Chemical Laboratory, Duke University, Durham, North Carolina 27706.
Received December 1, 1981

ABSTRACT: Monte Carlo folding simulations are performed with a bcc lattice model of pancreatic trypsin inhibitor. We compare the results obtained with centrosymmetric and local interaction potentials in five folding runs with different sets of random numbers. The four initial structures investigated are the best lattice representation of the native molecule, a random coil, a randomized structure having the disulfide bonds intact, and one having the helix intact. Both potentials result in smooth folding to globular conformations having root-mean-square deviations equivalent to, or smaller than, those previously obtained by similar methods using multifactor potentials. This observation is ascribed to restriction of the available conformational space by the lattice model. The indices used to compare the generated and idealized native structures indicate no preference between the two types of folding potentials. Retention of the correct disulfide bonds in the starting structure strongly directs folding toward the native conformation.

Introduction

Attempts to predict the native conformation of a protein molecule by minimization of an empirical energy function, using a multiatom representation of each residue, have foundered due to the existence of multiple minima in the energy surface.[1,2] This failure led to the exploration of highly simplified models of the peptide chain for folding simulations based upon Monte Carlo techniques. Levitt and Warshel[3] pioneered the use of simplified models, using as a test structure the small, single subunit protein pancreatic trypsin inhibitor (PTI). In the first of these papers, each of the $N = 58$ residues that is not glycine is replaced by two spheres taken to represent the peptide backbone and side chain, respectively. The bonds of this model chain are the virtual bonds connecting α-carbon atoms, and the torsion angle, α_i, is determined by the coordinates of the four contiguous α-carbon atoms $i - 1$ to $i + 2$. A conformation corresponding to minimum energy is sought by molecular dynamics techniques, taking the $N - 4$ values of the torsional angles as independent variables. During their folding simulations, "thermalizations" were performed periodically to allow the conformation to escape local minima, and the course of the process could be guided by application of "holding" and "pushing" potentials.[4] The basic argument advanced by these authors is that the computer requirements for simulation can be reduced to manageable bounds, and the energy surface will contain fewer subsidiary minima, if the number of independent variables is restricted by simplifying the model. A somewhat similar procedure was subsequently used by Kuntz, Crippen, Kollman, and Kimelman,[5] although they adopted $3N$ Cartesian coordinates as independent variables, where N is the number of residues in the molecule. Robson and Osguthorpe[6] performed folding simulations using an angular variable, γ, which couples the variation of ϕ and ψ of the same residue. They applied the equivalent of Levitt and Warshel's "holding" and "pushing" potentials, but at regular intervals during the simulation.

The use of simplified models in folding simulations is based upon the assumption that the empirical energy function corresponds to an energy surface having a global minimum and that the conformation corresponding to this global minimum will closely resemble the "idealized" native state. Hence, these structures have been compared with the idealized native conformation using a root-mean-square deviation of distances. Claims of success for this type of

† Permanent address: Department of Chemistry, North Carolina Central University, Durham, N.C.

0024-9297/82/2215-1135$01.25/0